Results in Physics 7 (2017) 493–497

Contents lists available at ScienceDirect

Results in Physics

journal homepage: www.journals.elsevier.com/results-in-physics

Response surface modeling of photogenerated charge collection of silver-based plasmonic dye-sensitized solar cell using central composite design experiments

Samaila Buda [a,*], Suhaidi Shafie [a,b], Suraya Abdul Rashid [a,c], Haslina Jaafar [b], Ali Khalifa [b]

[a] Institute of Advanced Technology, Universiti Putra Malaysia, 43400 UPM Serdang, Selangor Darul Ehsan, Malaysia
[b] Department of Electrical and Electronics Engineering, Faculty of Engineering, Universiti Putra Malaysia, 43400 UPM Serdang, Selangor Darul Ehsan, Malaysia
[c] Department of Chemical Engineering, Faculty of Engineering, Universiti Putra Malaysia, 43400 UPM Serdang, Selangor Darul Ehsan, Malaysia

ARTICLE INFO

Article history:
Received 12 November 2016
Received in revised form 5 January 2017
Accepted 5 January 2017
Available online 10 January 2017

Keywords:
Modeling
Solar cell
Optimization
Plasmonic

ABSTRACT

In this study, silver nanoparticles (AgNP) have been prepared and successfully incorporated in TiO_2 nanopowder and used in dye-sensitized solar cell as photoanode. The effect of the AgNP concentration and photoanode film thickness on the charge collection efficiency of a photogenerated electron at the external circuit was investigated using response surface methodology. A multiple regression analysis of second order polynomial was employed to fit the experimental data and an empirical model was subsequently developed using analysis of variance (ANOVA). The results show that two independent variables (AgNP concentration and photoanode film thickness) have significantly influenced the charge collection efficiency of the silver-based plasmonic DSSC. An optimum charge collection of 64.3% was obtained at AgNP concentration and film thickness of 5%wt and 10 μm, respectively.

© 2017 The Authors. Published by Elsevier B.V. This is an open access article under the CC BY-NC-ND license (http://creativecommons.org/licenses/by-nc-nd/4.0/).

Introduction

The Economic and social wellbeing of any nation or community are largely dependent on the extent of its energy utilization, thus, energy, fresh water, and air are considered as the most important commodities for human existence. Fossil fuels such as petroleum, natural gas, and coal are the most widely used sources of energy for industrial and domestic purposes. The depletion of the earth, fossil fuel reserves and environmental concern such as greenhouse gas emission are some of the drawbacks of these highly efficient carbon-based fuels [1]. Solar energy is a renewable source of energy that has attracted global attention as a substitute for the fossil fuels owing to its numerous advantages of being a naturally infinite commodity that is free from environmental pollution. Hence solar energy is indeed one of the most viable alternatives to consider in overcoming world's energy crisis.

Among the various solar photovoltaic cells, dye-sensitized solar cell (DSSC) has been considered as a promising solar cell device for solar electricity generation owing to its low cost, flexibility, ease of production, and low toxicity [2].Titanium dioxide (TiO_2) has been widely used in DSSC photoanode due to its large surface area which is beneficial in maximizing dye loading onto the semiconductor surface [3]. The modification of TiO_2 with a metal nanoparticles such as gold (Au), silver (Ag) [4] and platinum (Pt) has been widely reported to prevent the recombination of the photogenerated electron–hole pairs and improve the charge transfer efficiency in DSSC [5]. Silver nanoparticles have been utilized to improve photon absorption in the TiO_2-based DSSC photoanode because of its surface plasmon resonance effect which concentrates and then scatters the incoming solar radiation [6] which enhances light absorption by the sensitizing molecules.

In addition to their surface plasmon resonance effect, a noble metal to TiO_2 can also enhance the photovoltaic performances by changing the surface properties of the semiconductor, since the work function of the metal is higher than that of TiO_2, such that electrons are displaced from the TiO_2 in the vicinity of each metal particle which then create a Schottky barrier at each metal–semiconductor region, thereby decreases the charge recombination [7],

For high conversion efficiency to be achieved, there must be an efficient collection of nearly all the photogenerated electrons which means that the incident photon to- Current-efficiency should be close to unity under visible light region. This can be realized if the carrier diffusion length is greater than the film thickness [8].

Response surface methodology (RSM) is a resourceful statistical modeling tool that has been developed and used in testing process

* Corresponding author.
E-mail address: budasamaila@gmail.com (S. Buda).

http://dx.doi.org/10.1016/j.rinp.2017.01.011
2211-3797/© 2017 The Authors. Published by Elsevier B.V.
This is an open access article under the CC BY-NC-ND license (http://creativecommons.org/licenses/by-nc-nd/4.0/).

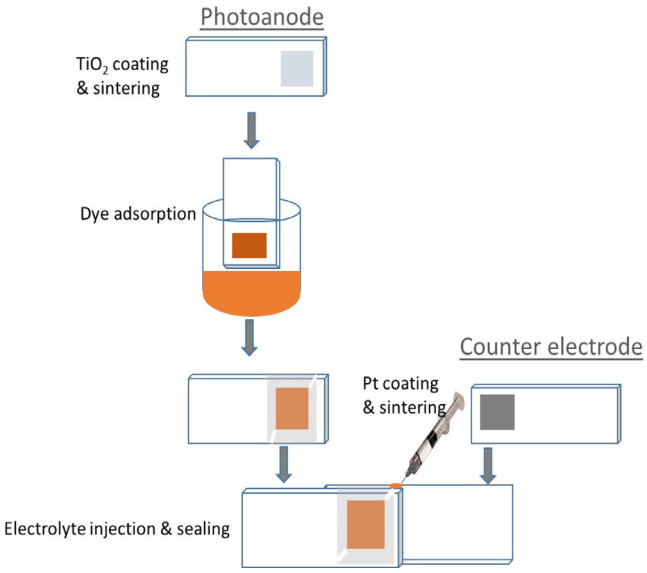

Fig. 1. DSSC fabrication process.

parameters and their effects on the resulting output in a given experiment [9], RSM is used in design optimization in order to reduce the cost of expensive analysis methods such as finite element method and computational fluid dynamic analysis and their attendant numerical noise. Additionally the problem can be estimated with smooth functions that increase the convergence of the optimization process because they reduce the effects of noise which allow for the use of derivative-based algorithms. This mathematical technique can also be used in developing an approximately accurate prediction of system throughput and subsequent development of a mathematical model that can exactly describe the overall process [10], the developed model identifies the links between various operational factors and their individual responses with multiple ideal criteria by determining the influence of these effective parameters on the coupled output variables, thereby minimizing the experimental costs and more importantly, reducing the inconsistency around the expected result [11].

In this research, a mathematical model has been developed based on several experimental trials in order to gain an insight on the influence of film thickness and concentration of silver nanoparticles on the collection efficiency of the photogenerated electron in DSSC. To realize this objective, a central composite design (CCD) based on the polynomial model of quadratic order was employed where each factor is varied over five levels for efficient design optimization. Subsequently, the model was fortified through regressive analysis and examination by analysis of variance (ANOVA) technique to minimize error thereby improving its resultant accuracy.

Materials and methods

Materials

Titanium dioxide (TiO_2), Flourine Tin oxide (FTO) coated glass ($7sq^{-1}$), Di-2 Cis-bis (isothiocyanato) bis-bipyridyl-4-4′-dicarboxy lato) ruthenium (II) (N719) dye were obtained from Sigma-Aldrich Co., (USA). Silver nitrate was purchased from Qrec chemicals, and liquid electrolyte was obtained from Kyutech Laboratory, Japan

Methods

Silver nanoparticles were synthesized according to the procedure reported by Silvert et al. [12] Firstly, 4 g of polyvinylpyrrolidone(PVP) was dissolved in 50 mL ethylene glycol at room temperature, also 100 mg $AgNO_3$ was added to this solution. The resultant suspension was stirred using magnetic stirrer for 30 min. thereafter, the solution was put in a Teflon autoclave and heated in a furnace at 120 °C for 6 h and allowed cooling to room temperature, the PVP, and the solvent were removed by centrifugation. Secondly, TiO_2/Ag paste was obtained by mixing a required amount of the AgNP with 2g TiO_2 powder in ethanolic solution of ethyl cellulose.

TiO_2/Ag layer was deposited on FTO-coated glass substrates by screen printing technique followed by drying at 100 °C in an oven. The desired film thickness (from 5 μm to 30 μm) was achieved by reperative coating, the obtained films were sintered in a furnace at 450 °C for 30 min. A monolayer dye coating of the electrodes was achieved by immersing the films in a 0.2 mM ethanolic solution of N719 for 12 h. The counter electrodes were fabricated by coating a platinum paste on a pre-drilled FTO glass substrates by screen printing followed by sintered 400° for 30 min. The dye-loaded photoanode and the Pt-counter electrodes were assembled together sandwiched by 60 μm surlyn polymer sheet. The assembled devices were heated on a hot plate until the two electrodes were firmly glued together. Finally, liquid electrolyte was administered into the device through the drilled holes at the counter electrode and then sealed with a polymer sheet (Fig. 1).

Determination of charge transfer process

Electrochemical impedance spectroscopy (EIS) was carried out on the DSSCs using Autolab PGSTAT204, the electrochemical impedance spectra were measured in the frequency range between 0.01 Hz and 100KHz The series resistance (R_s) of the cell was deduced from the Nyquist plot (Fig. 4.) as the point of intercept of the semicircle on the x-axis while the charge transfer resistance (R_{ct}) at the dye/electrolyte interface is the value of the arc length of the semicircle [13]. Electrochemical impedance data represented in a Bode phase plot was used for the determination of maximum frequency, here, the log of the frequency is plotted on the x-axis

Table 1
Comparison of photovoltaic performance of some plasmonic $DSSC_s$.

Photoanode	NP synthesis method	J_{sc} (mA cm^{-2}	V_{oc} (V)	FF	?? (%)	Refs.
TiO_2-Ag	Chemical reduction	8.4	0.63	51	2.7	[15]
TiO_2-Ag	Chemical reduction	12.19	0.77	0.52	4.86	[16]
Au-Ag/TiO_2	Chemical reduction	23.5	0.76	0.41	7.33	[17]
Ag-TiO_2	Thermal evaporation	10.0	0.62	0.41	2.55	[18]
Al-TiO_2	Solution process	17.6	0.72	0.56	6.95	[19]
Ag/TiO_2	Photoreduction	16.2	0.76	–	8.9	[20]
TiO_2-Ag	Biosynthesis	11.80	0.79	0.55	5.12	[21]

Table 2
Independent Variable coded levels.

Factor	Name	Level		
		Low	Centre	High
X_1	Amount of silver NP (%wt)	0	5	10
X_2	Film Thickness (μm)	5	12.2	30

Table 3
Central composite experimental design matrix for the two independent variables.

Run	AgNP (wt%)	Film (μm)	Charge collection (%)
1	5	25	45
2	7.5	20	38
3	0	30	32
4	5	15	63
5	5	10	65
6	5	20	41
7	6.5	30	30
8	10	5	48
9	2.5	10	62
10	5	30	40
11	0	5	45
12	6	20	35
13	2.5	15	42

and the phase shift on the y-axis. The maximum frequency(ω_{max}) was traced from the graph and the electron life time(τ_n) was calculated from relation [14].

$$\tau_n = 1/2\pi f \quad (1)$$

Using τ_n and R_{ct} deduced from the Nyquist plot, chemical capacitance was obtained from the equation below (Table 1).

$$\tau_n = R_{ct}C_\mu \quad (2)$$

Similarly, the electron transport time τ_s is given as,

$$\tau_s = R_sC_\mu \quad (3)$$

Experimental design

Central composite Design (CCD) is a center point factorial design method incorporated in a response surface methodology employed for efficient modeling of an independent variable with curvature through augmentation of some points to the previously performed design. A design-Expert software version 6.0.6 was used to assign two independent variables namely, Amount of silver nanoparticles (%wt) and film thickness (μm) on five level points as shown in Table 2, this resulted in 13 experimental sets as represented in equation below and shown in Table 3.

$$\text{Number of experiment} = 2^k + 2k + 3 \quad (4)$$

where k is the number of independent variables.

The relationship between the variable factors X_1, X_2, and the response Y is written as follows.

$$Y = F(X_1X_2) \quad (5)$$

where F represent the response function.

In this case, a polynomial model based on Taylor's expansion series is chosen and represented below [22].

$$Y = bo + \sum_{i=1}^{k} bixi + \sum_{j}^{k} bijxixj(i,j = 1,2,\ldots..,k) + e \quad (6)$$

Putting the predicted solar cell efficiency Y and the variables X_1 and X_2 representing the amount of silver nanoparticles and film thickness respectively, Eq. (6) becomes.

$$f(x) = \beta_0 + \beta_1X_1 + \beta_2X_2 + \beta_{12}X_1X_2 + \beta_{13}X_1X_3 \quad (7)$$

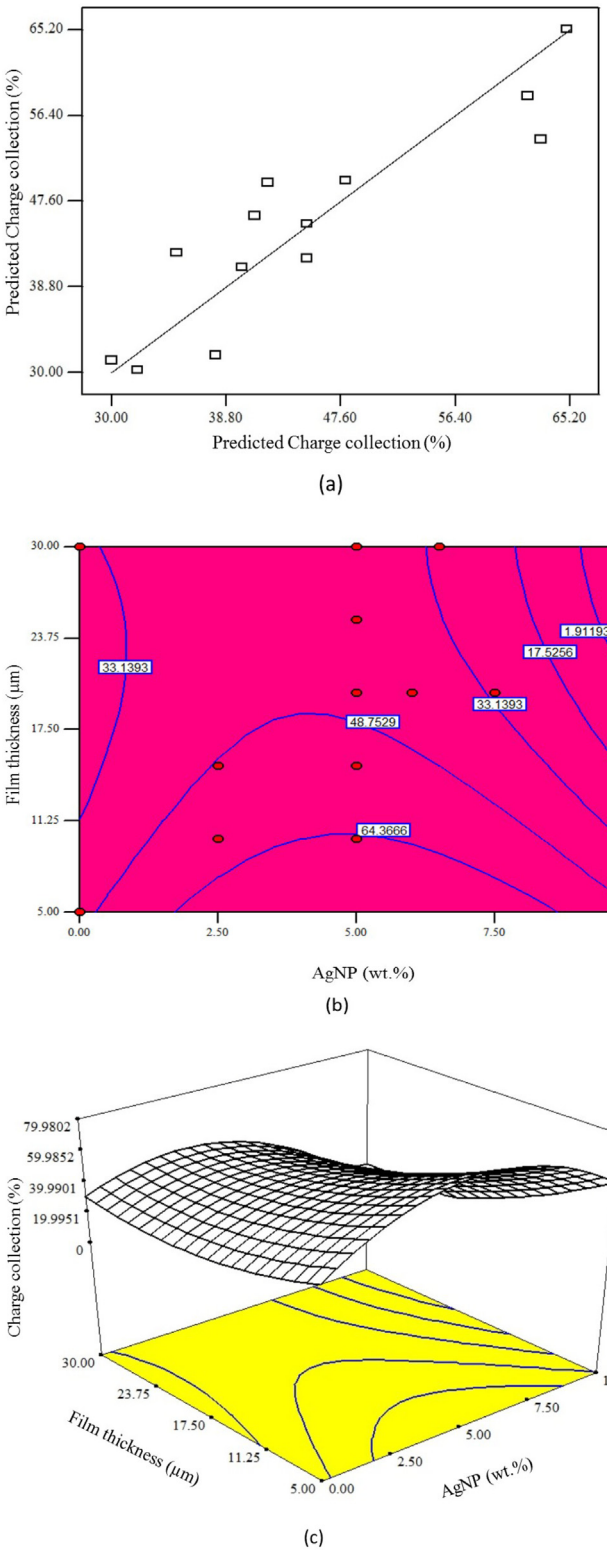

Fig. 2. Response surface for charge collection as a function of AgNP concentration and film thickness.

Results

Development of the regression model

Having performed all 13 experiment outlined in the design matrix in Table 3 above, a carefully selected regression model

Table 4
Summary of statistical parameters for the ANOVA regression model.

Source	Quadratic
Adequate precision	8.007
Coefficient of variance	14.25
R^2	0.8221
Adjusted R^2	0.6933
Sum of Squares	1.12
Degrees of freedom	3
Mean square	0.37
F value	6.43

based on the highest order polynomial was developed. The relationship between the charge collections efficiency (Y) represented as the dependent variable and the independent variables X_1 and X_2 represent the amount of silver and film thickness respectively are computed through multiple regression fitting of the experimental results, this empirical model is represented in the Eq. (8) below.

$$\text{Charge collection } (\%) = 58.64825 + 14.42008X_1 - 3.02960X_2 - 1.3006X_1^2 + 0.069437X_2^2 - 0.19366X_1X_2 \quad (8)$$

the linear terms X_1 and X_2 represent the effect of the individual variable on the charge collection while the multiple of the variable terms shows the interaction of the independent variables on the response and the quadratic effect was represent by the squares of the terms.

Adequacy of the model

Analysis and subsequent optimization of the fitted empirical model were carried out to ensure an efficient approximation of the actual values as well as to avoid distorted result [23]. The predicted versus actual efficiency plot is shown in Fig. 2a, from the plot, it is clear that the predicted values were considerably similar to the experimental values of the charge collection efficiency of the fabricated DSSC, the coefficient of determination (R^2) are calculated to be equals to 0.8221 and this shows that only 0.1779% of the entire variation was not predicted by the empirical model. Furthermore, this healthy correlation between the predicted and actual charge collection efficiency indicates the effectiveness of the developed model. The model accurate precision (AP) value which is the extent of signal noise is 8.007 this indicates an adequate signal in the obtained model. It can be seen from the contour plot in Fig. 2b, that the incremental addition of AgNP from 2.0%wt to 8%wt with the corresponding film thickness range between 5 μm and 10 μm results in a linear rise in charge collection from a modest 48% up to about 64%. However, further increase of AgNP was accompanied by sharp decrease in charge collection which may be due to a decrease of shunt resistance caused by high concentration of metallic particles [24].

Fig. 2c present the 3D-plot of charge collection efficiency of the silver-based plasmonic DSSC, it clearly shows that an efficient charge collection could be achieved at AgNP concentration range between 2.00%wt and 8.00%wt with the corresponding photoanode film thickness range from 5 m to 10 m, this confirms the accuracy of the developed model (Tables 4 and 5).

The equivalent circuit model for the EIS studies is shown in Fig. 3, it present the relationship between the electron transport resistance Rt (= r_t L), the recombination resistance Rr (=r_r L) and the TiO_2 layer thickness L [25]. The physical meaning is that reduction of film thickness will significantly reduce the electron transport resistance as well as increase recombination resistance in the cell device and as a result, efficient charge collection is achieved at the cell/external circuit interface.

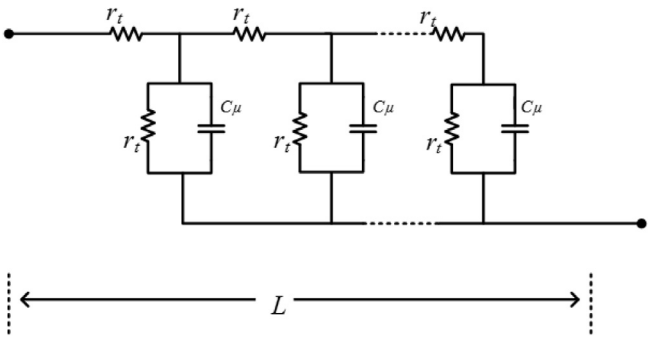

Fig. 3. Equivalent circuit model of DSSC.

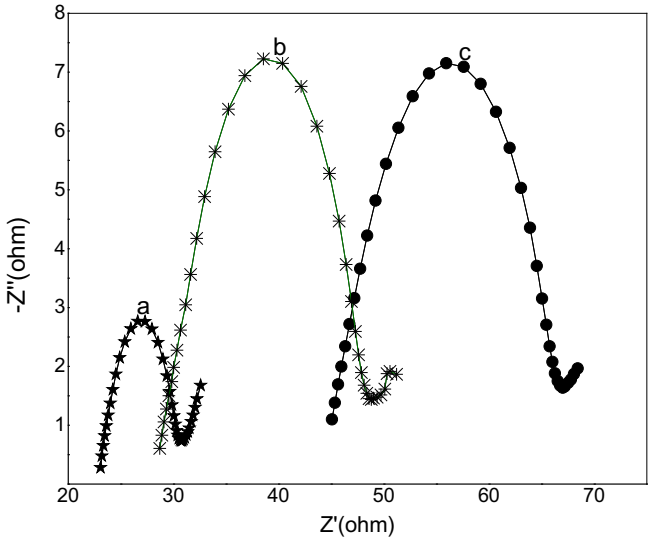

Fig. 4. Nyquist plot of (a) Bare TiO_2 (b) Ag/TiO_2 1% and (c) Ag/TiO_2 10%.

Table 5
Analysis of Variance (ANOVA) and lack of fit test response of the developed quadratic model.

Source	Sum of squares	Degree of freedom	Mean squares	F value	Prob >F
Model	1326.05	5	265.21	6.43	0.015
X_1	228.38	1	228.38	5.53	0.0509
X_1	1187.2	1	1187.2	28.77	0.001
X_1	568.65	1	568.65	13.78	0.0075
X_2^2	125.03	1	125.03	3.03	0.1253
X_1X_2	250.71	1	250.71	6.08	0.0432
Residual	288.88	7	41.27		

Solar cell characterization

Electrochemical impedance spectroscopy (EIS) was carried out to investigate the interfacial charge transfer process of the solar cell. The data was recorded in the frequency range from 0.01 Hz to 100 Hz. On the Nyquist plot, the intersection of the semicircle at the real axis represents the series resistance of the device (Rs) while the arc length of the semicircle represents the charge transfer resistance (R_{ct}) between the dye-adsorbed photoanode and the electrolyte interface.

The Nyquist plot as shown in Fig. 4a shows a high sheet resistance Rs of 44Ω for bared TiO_2 based DSSC. Upon addition of AgNP, the resistance reduced to 28Ω and further to 22Ω for cells with 1% and 10% AgNP concentration as shown in Fig. 4b and Fig. 4c respectively. Furthermore, R_{ct} of the bared TiO_2–based DSSC increases from 9Ω to 22Ω upon addition of AgNP (10 wt%). This rise in the R_{ct} value could lead to a higher open-circuit voltage (V_{oc}) and fill factor (FF) of the DSSC device as a result of a reduction in recombination between electrons in the TiO_2 and the hole in the electrolyte [16], this result supports the ANOVA regression analysis of the empirical model [26].

Conclusion

Central composite design was successfully employed to study and establish relationships between process variable such as AgNP concentration and film thickness and the collection of photogenerated electrons in the silver-based plasmonic dye-sensitized solar cell. The electron collection efficiency as a function of silver nanoparticle concentration and film thickness for Ag/TiO_2 plasmonic dye-sensitized solar cell was successfully developed and optimized using ANOVA for high accuracy prediction. The solar cell with 5 wt% of AgNP and 10 μm film thickness has shown the highest charge collection efficiency of 64.3%.

Acknowledgements

This research work was fully sponsored by a Universiti Putra Malaysia grant (GP-IPS/2015/9459600).

References

[1] Şen Z. Solar Energy Fundamentals and Modeling Techniques: Atmosphere, Environment, Climate Change and Renewable Energy. Springer; 2008.
[2] Jena A, Mohanty SP, Kumar P, Naduvath J, Gondane V, Lekha P, et al. Dye sensitized solar cells: a review. Trans Indian Ceram Soc 2012;71(1):1–16.
[3] Roy P, Kim D, Lee K, Spiecker E, Schmuki P. TiO_2 nanotubes and their application in dye-sensitized solar cells. Nanoscale 2010;2(1):45–59.
[4] Lim SP, Pandikumar A, Huang NM, Lim HN. Silver/titania nanocomposite-modified photoelectrodes for photoelectrocatalytic methanol oxidation. Int J Hydrogen Energy 2014;39(27):14720–9.
[5] Lim SP, Pandikumar A, Lim HN, Ramaraj R, Huang NM. Boosting photovoltaic performance of dye-sensitized solar cells using silver nanoparticle-decorated N, S-Co-doped-TiO_2 photoanode. Sci Rep 2015;5:11922.
[6] Photiphitak C, Rakkwamsuk P, Muthitamongkol P, Sae-Kung C, Thanachayanont C. Effect of silver nanoparticle size on efficiency enhancement of dye-sensitized solar cells. Int J Photoenergy 2011;2011:1–8.
[7] Pandikumar A, Lim S-P, Jayabal S, Huang NM, Lim HN, Ramaraj R. Titania@gold plasmonic nanoarchitectures: An ideal photoanode for dye-sensitized solar cells. Renewable Sustainable Energy Rev 2016;60:408–20.
[8] Grätzel M. Solar energy conversion by dye-sensitized photovoltaic cells. Inorg Chem 2005;44(20):6841–51.
[9] John G, Sangamithra A, Chandrasekar V. Dyes and Pigments Response surface modeling and process optimization of aqueous extraction of natural pigments from Beta vulgaris using Box e Behnken design of experiments. Dyes Pigm 2014;111:64–74.
[10] Ramimoghadam D, Bagheri S, Yousefi AT, Hamid SBA. Statistical optimization of effective parameters on saturation magnetization of nanomagnetite particles. J Magn Magn Mater 2015;393:30–5.
[11] Rout SK, Hussein AK. Multi – objective optimization of a three-dimensional internally finned tube based on Response Surface methodology (RSM). J Therm Eng 2015:131–42.
[12] Silvert P-Y, Herrera-Urbina R, Duvauchelle N, Vijayakrishnan V, Elhsissen KT. Preparation of colloidal silver dispersions by the polyol process. Part 1—Synthesis and characterization. J Mater Chem 1996;6(4):573–7.
[13] van de Lagemaat J, Frank AJ. Effect of the surface-state distribution on electron transport in dye-sensitized TiO_2 solar cells: nonlinear electron-transport kinetics. J Phys Chem B 2000;104:4292–4.
[14] Kim SG, Ju MJ, Choi IT, Choi WS, Choi HJ, Baek JB, et al. Nb-doped TiO_2 nanoparticles for organic dye-sensitized solar cells. RSC Adv 2013;3(37):16380.
[15] Berginc M, Krašovec UO, Topič M. Solution processed silver nanoparticles in dye-sensitized solar cells. J Nanomater 2014;2014:49–56.
[16] Lim SP, Pandikumar A, Huang NM, Lim HN. In-situ electrochemically deposited polypyrrole nanoparticles incorporated reduced graphene oxide as an efficient counter electrode for platinum-free dye-sensitized solar cells. RSC Adv 2014;4(i):38111–8.
[17] Lim SP, Lim YS, Pandikumar A, Lim HN, Ng YH, Ramaraj R, et al. Gold–silver@TiO_2 nanocomposite-modified plasmonic photoanodes for higher efficiency dye-sensitized solar cells. Phys Chem Chem Phys 2017;353(i):737–40.
[18] Haidari G, Hajimahmoodzadeh M, Fallah HR, Peukert A, Chanaewa A, Von Hauff E. Thermally evaporated Ag nanoparticle films for plasmonic enhancement in organic solar cells: effects of particle geometry. Phys Status Solidi RRL 2015;165(3):161–5.
[19] Xu Q, Liu F, Liu Y, Meng W, Cui K, Feng X, et al. Aluminum plasmonic nanoparticles enhanced dye sensitized solar cells. Opt Express 2014;22(Suppl. 2):A301–10.
[20] Jeong NC, Prasittichai C, Hupp JT. Photocurrent enhancement by surface plasmon resonance of silver nanoparticles in highly porous dye-sensitized solar cells. Langmuir 2011:14609–14.
[21] Tian HYZ, Wang L, Jia L, Li Q, Song Q. A novel biomass coated Ag-TiO_2 composite as a photoanode for enhanced photocurrent in dye-sensitized solar cells. RSC Adv 2013;3:6369–76.
[22] Khuri AI, Mukhopadhyay S. Response surface methodology. Wiley Interdiscip Rev Comput Stat 2010;2(2):128–49.
[23] Diwaniyan S, Sharma KK, Kuhad RC. Laccase from an alkalitolerant basidiomycetes Crinipellis sp. RCK-1: Production optimization by response surface methodology. J Basic Microbiol 2012;52(4):397–407.
[24] Subramanian V, Wolf EE, Kamat PV. Catalysis with TiO_2/Gold nanocomposites. Effect of metal particle size on the fermi level equilibration. J Am Chem Soc 2004;126(15):4943–50.
[25] Sarker S, Seo HW, Kim DM. Calculating current density-voltage curves of dye-sensitized solar cells: A straight-forward approach. J Power Sources 2014;248:739–44.
[26] Lim SP, Pandikumar A, Huang NM, Lim HN, Gu GC, Ma TL. Promotional effect of silver nanoparticles on the performance of N-doped TiO_2 photoanode-based dye-sensitized solar cells. RSC Adv 2014;4(89):48236–44.